

# Clues on the nature of Compact Steep Spectrum radio sources from optical spectroscopy

R. Morganti<sup>1,2</sup>, C.N. Tadhunter<sup>3</sup>, R. Dickson<sup>3</sup>, and M. Shaw<sup>3</sup>

<sup>1</sup> Australia Telescope National Facility, CSIRO, PO Box 76, Epping, NSW 2121, Australia

<sup>2</sup> Istituto di Radioastronomia, CNR, via Gobetti 101, I-40129 Bologna, Italy

<sup>3</sup> Department of Physics, University of Sheffield, Sheffield S3, UK

Received 28 January 1997 / Accepted 9 April 1997

**Abstract.** New long-slit spectra are presented for a group of Compact-Steep-Spectrum (CSS) sources (i.e. powerful radio sources with sub-galactic size and steep spectral index at high radio frequencies) selected from the southern ( $\delta < 10^\circ$ ) 2-Jy sample of radio sources with redshift limit of  $z = 0.7$ . Their spectra are strong in emission lines (e.g. [O III] $\lambda$ 5007 and [O II] $\lambda$ 3727), as expected for such powerful radio sources. The line luminosities and ratios obtained for these compact sources are compared with those for the other sources of the southern 2-Jy sample. We find that the optical spectra for the CSS sources show characteristics very similar to the extended sources of similar radio power and redshift. In particular, we find that the CSS sources follow the correlation between the radio power and [O III] $\lambda$ 5007 and [O II] $\lambda$ 3727 luminosities found for the extended sources, although there is tentative evidence that they have lower [O III] $\lambda$ 5007 luminosities. Also, the optical continuum spectral energy distribution (SED) and polarization properties of the CSS sources show the same variety of characteristics observed among the extended sources. The first-order similarity that we find between the spectra of CSS sources and the extended sources of similar radio power is consistent with the idea that the CSS sources are young radio sources in which the radio jets have yet to emerge from the central regions of the host galaxies.

**Key words:** galaxies: active – galaxies: nuclei – radio continuum: galaxies

---

## 1. Introduction

Powerful radio sources with sub-galactic size and steep spectral index at high radio frequencies (i.e. Compact Steep Spectrum

(CSS) sources)<sup>1</sup> are believed to represent either the young phase of powerful extragalactic radio sources (the “youth” scenario: Readhead *et al.* 1995; Fanti *et al.* 1995; Readhead 1996 and ref. therein), or sources trapped by unusual conditions of their interstellar medium (ISM), that prevent them from growing to normal dimensions (the “frustration” scenario e.g. Phillips & Mutel 1982; van Breugel 1984). Either of these hypothesis make these objects extremely interesting and very important for our understanding of radio sources in general.

A typical CSS source is a powerful radio source (usually  $\log P_{\text{tot}} > 10^{26} \text{ W Hz}^{-1}$  at 2.7 GHz, Fanti & Fanti 1994), but with a size much smaller than – or at most comparable with – the optical galaxy-scale ( $D < 30 \text{ kpc}$ ) and a steep high-frequency radio spectrum. According to early studies of Fanti *et al.* (1990), the small size of the CSS cannot be explained as a projection effect, because the observed number of CSS sources is too large. A lot of work has been done in studying these objects at radio wavelengths and a summary of the typical characteristics and parameters is given in Fanti & Fanti (1994 and refs therein). Most of these sources show a symmetric, double-lobed structure characteristic of the more extended FR II radio sources (Fanti *et al.* 1990; Spencer *et al.* 1991; Dallacasa *et al.* 1994; Readhead 1996 and references therein), with no dominant flat spectrum core. Therefore, they can easily be seen as down-scaled version of large powerful radio galaxies. Fanti *et al.* (1995) have recently investigated whether the conditions of the external ISM around CSS sources can be such to confine these sources and keep them small. They conclude that this is not the case and they support the idea of CSS sources as the young phase of large radio sources. However, the existing optical and X-ray data available are limited, and more data are needed to confirm their results.

Recently, a complete sample of powerful radio sources has been observed and studied across the electromagnetic spectrum (see Morganti *et al.* 1995 for a summary). Although dominated

---

<sup>1</sup> This definition also includes Gigahertz-Peaked sources (GPS) which have spectra peaked at GHz frequencies and are believed to be smaller than the CSS sources

by large-scale extended radio sources, this sample also includes a group of CSS sources. In this paper we will investigate in some detail the characteristics of the optical spectra of these CSS sources and compare them with those of the rest of the sample (that are mainly FRII radio sources). A major advantage of this study over previous work is that we can compare well-defined, complete samples of CSS sources and extended radio sources over a *similar range of redshift and radio power*.

The paper is organized in the following way. In Sect. 2 we present the sample that we are using for our study, in Sect. 3 we describe the new optical observations carried out for the CSS sources in the sample. In Sect. 4 we summarise the main characteristics of the optical spectra of CSS sources. Finally, in Sect. 5 a comparison between the luminosity of the optical lines and the line ratios for CSS and extended sources will be done and the implications will be discussed in Sect. 6.

## 2. The sample

The group of CSS sources considered in this study is selected from a complete sub-sample of the Wall & Peacock (1985) 2 Jy sample. This sub-sample consists of 88 radio sources (radio galaxies and quasars) having  $S_{2.7\text{GHz}} > 2.0$  Jy,  $\delta < 10^\circ$  and  $z < 0.7$ . Recently, this sample has been studied in detail at various wavelengths and a database of optical, radio and X-ray data is available (Tadhunter *et al.* 1993; Morganti *et al.* 1993, 1997; Siebert *et al.* 1996).

Following the definition of Fanti *et al.* (1995), we consider as CSS a source with high-frequency steep spectral index  $\alpha > 0.5$  (with  $S = \nu^{-\alpha}$ ) and linear dimensions<sup>2</sup>  $\leq 30$  kpc. We find 11 sources in our sample that match this definition. Four of these (0045-25 (NGC 253), 0453-20, 1246-41 (NGC 4690) and 1514+07 (3C317)) have a radio power much lower than the typical power of the CSS sources (i.e.  $\log P_{\text{tot}}(2.7\text{GHz}) \ll 26.0$ ). In particular, NGC 253 is a classic starburst galaxy and has a radio power which is orders of magnitude below that of most of the low redshift objects in the sample. The possibility of having low-redshift and low-power CSS sources has been discussed in Cotton *et al.* (1995) in the case of 4C31.04. However, here we will consider only the 7 objects with higher radio power  $\log P_{\text{tot}}(2.7\text{GHz}) > 26.0$  W Hz<sup>-1</sup> for the following two reasons: this will make the selection consistent with previous works of Fanti *et al.* (1990) and Spencer *et al.* (1991), and the optical information for the rest of the 2-Jy sample is more complete at the high radio power end (see Tadhunter *et al.* 1993). Thus, the radio power selection makes the comparison between CSS and extended sources more reliable.

The 7 CSS sources are listed in Table 1 together with information on the radio characteristics. All the sources have steep high frequency spectra (data taken from King, 1994), although PKS1934-63 is formally classified as a Gigahertz Peak Source (GPS) on the basis of its spectral turnover at 1GHz. A detailed study of these objects at radio wavelengths will be presented in a forthcoming paper (Tzioumis *et al.* in prep.), but VLBI maps

**Table 1.** List of the objects with a summary of their characteristics

Name	Type	$m_V$	$z$	$\log P_{5\text{GHz}}$ W Hz <sup>-1</sup>	Lin. Size kpc
0023 – 26	G/CSS	19.5	0.322	27.28	4.06
0252 – 71	G/CSS	20.9	0.563	27.59	1.55
1151 – 34	Q/CSS	17.8	0.258	26.98	0.49
1306 – 09	G/CSS	20.5	0.464	27.37	2.72
1814 – 63	G/CSS	18.0	0.063	25.90	0.50
1934 – 63	G/GPS	18.4	0.183	27.04	0.17
2135 – 20	G/CSS	19.4	0.635	27.59	1.37

Explanation of Columns - (1) IAU designation for object. (2) Q = quasar, G = galaxy. (3) Apparent visual magnitude. (4) redshift. (5) Radio power at 5 GHz (Morganti *et al.* 1993). (6) Linear size of the radio emission (Tzioumis *et al.* in prep.).

of the 7 sources studied in this paper can be found in Tzioumis *et al.* (1996) and King *et al.* (1993, 1996). The radio data available show that the sources (with possibly one exception, 1814-63) have a double structure (i.e. two symmetric lobes), in agreement with what usually found for CSS sources (see Fanti *et al.* 1995; O’Dea *et al.* 1991).

Two of the sources in the sample exhibit broad lines in their optical spectra: 1151-34 (Tadhunter *et al.* 1993) and 2135-20 (Shaw *et al.* 1995). Of these two, 1151-34 was originally classified as a quasar on the basis of its optical appearance (Wall & Peacock 1985), whereas its optical luminosity is more consistent with that of a broad line radio galaxy ( $M_v > -23$ , Veron-Cetty & Veron 1993). On the other hand, 2135-20 presents the reverse case: it was originally classified as a galaxy on the basis of its optical appearance, but its optical luminosity falls at the lower end of the quasar range ( $M_v < -23$ , Veron-Cetty & Veron 1993). Since neither of these objects is highly polarized at optical/UV wavelengths (see below), it is likely that they are both genuine broad line objects in which the nuclei are seen directly rather than by scattered light.

## 3. The new optical data

Low-dispersion spectra for the complete sample of radio sources described above (i.e. including the extended sources), are presented in Tadhunter *et al.* (1993). There, the [O III] $\lambda$ 5007 luminosities are given for the majority of the objects while, for technical reasons, the information about the [O II] $\lambda$ 3727 luminosities is incomplete for the low redshift objects. For the CSS sources the information available from that paper was also not complete. Because of this we have reobserved five of the 7 CSS sources in two observing runs at the ESO 3.6-m telescope in La Silla (Chile) using the ESO Faint Object Spectrograph and Camera (EFOSC) in July 1993 and July 1994. The log of the observations is presented in Table 2.

For two objects (0023-26, 1306-09) the low dispersion spectra give a complete coverage of the observed wavelength range 3600Å to 8000Å. For 2135-20 only a spectrum in the blue was obtained during the same run. The seeing for most of the ex-

<sup>2</sup>  $H_0 = 50$  km s<sup>-1</sup>Mpc<sup>-1</sup>,  $q_0 = 0.0$

**Table 2.** Log of spectroscopic observations

Name	Date	Telescope	Instrument	Slit Width arcsec	Slit p.a. degrees	Grism/Arm	Exp.Time sec
0023-26	22/23-Jul-93	ESO 3.6-m	EFOSC	2	270	R300,B300	900
0252-71	11/12-Jul-94	ESO 3.6-m	EFOSC	5	270	R300,B300	900,600
1306-09	22/23-Jul-93	ESO 3.6-m	EFOSC	2	270	R300,B300	900
1934-63	11/12-Jul-94	ESO 3.6-m	EFOSC	2	270	B300	1200
2135-20	22/23-Jul-93	ESO 3.6-m	EFOSC	2	270	B300	1200
2135-20	23/24-Jul-93	WHT 4.2-m	ISIS	2	343	red,blue	4×1200,3×1200

posures was in the range 1.3'' to 1.8'' (FWHM). However, for 0252-71 and 1934-638 the spectra were taken in moderate/poor seeing (2 - 2.2'', FWHM).

As well as the data collected with the ESO 3.6-m telescope, spectra of 2135-20 were obtained using the 4.2-m William Herschel Telescope on the La Palma with the red and blue arms of ISIS spectrograph. The spectra were taken in moderate/poor seeing conditions (2''). The slit was oriented with a position angle of 343° which was within ~ 20° of the parallactic angle.

Finally, in the case of 1814-63, the spectrum presented in Tadhunter *et al.* (1993) was affected by the presence of a strong nearby star. However, a more careful reduction of that spectrum has allowed to obtain a better estimation of the luminosity of the lines (in particular [O III]λ5007) although this spectrum remains of poorer quality.

In the same observing runs with the ESO 3.6-m telescope, we also obtained optical/UV polarimetry for some of the objects (0023-26, 1306-09, 1934-63 and 2135-20). In the case of 1934-638 and 2135-20 the results are presented in Tadhunter *et al.* (1994a) and Shaw *et al.* (1995) respectively. Optical polarization measurements of 1151-34 were obtained on the Anglo Australian Telescope as part of a programme of spectropolarimetry observations of southern quasars in February 1996.

## 4. Results

The new spectra and the re-analysed spectra of 1814-63 are shown in Figs 1 to 6 (while for the spectrum of 1151-34 we refer to Tadhunter *et al.* 1993). Table 3 lists the fluxes of all the lines we could measure in each spectrum. Note that (except for 1814-63), prior to the measurement of the line fluxes, the continuum spectral energy distribution (SED) was modelled in terms of an elliptical galaxy template and a power-law (see Dickson 1997 for details), and the model continuum was then subtracted from the spectrum. The subtraction of the stellar continuum is important for the measurement of diagnostic emission lines.

The spectra of the CSS sources in this sample are rich in strong emission lines, as expected for such powerful radio sources. The spectra are characterized by the presence of strong [O III]λ5007 and [O II]λ3727 lines (as well as Hα+[N II]λλ6548, 84 for the objects for which the red part of the spectra is available). Weak Hβ is observed in all but two objects. However, the fact that we do not observe Hβ in 1814-63 is likely to be due to some contamination still present from the

nearby star, while this line is not measured in 0252-71 because it falls in one of the atmospheric absorption bands.

Some of the CSS sources in our sample have spectra of low or moderate ionization. In two objects (0023-26 and 1306-09), in fact, the [O II]λ3727 is stronger than [O III]λ5007. Note that the high ionization line HeIIλ4686 is either weak or absent in most of the spectra, although [NeV]λ3426 is observed in 0252-71, 1934-63 and 2152-20. We detect [NeIII]λ3869 and the blue doublet of [SII]λ4068 in most of the objects, but we have information on the red part of the spectra only for 0023-26 and 1306-09 (and less reliable for 1814-63). The [OI]λ6300 line appears to be relatively strong in both 0023-26 and 1814-63 and was also noted to be strong, compared to other radio galaxies, in 1934-63 by Penston & Fosbury (1978). Hγ+[OIII]λ4363 are also detected and in three cases (0023-26, 1934-63 and 2135-20) we could reliably deblend the two lines and estimate the temperature of the ionized gas (see below). For the other objects the values are too uncertain to estimate the temperature.

Recently, Gelderman & Whittle (1994) have presented spectroscopy of a heterogeneous collection of 19 CSS sources selected from Spencer *et al.* 1989. The redshift range for their radio galaxies is very similar to what we have in our sample, therefore allowing a comparison between the two. We find that the [O III]λ5007 fluxes in the objects observed by Gelderman & Whittle (1994) fall roughly in the same range of [O III]λ5007 flux (log F<sub>[OIII]</sub> between -14.7 and -13.32 erg s<sup>-1</sup>cm<sup>-2</sup>) as the values of our sample (see Table 3). The line ratio [O III]λ5007/Hβ is also similar in the two samples with a typical value for the radio galaxies in Gelderman & Whittle (1994) of [O III]λ5007/Hβ ~ 5. On the other hand, they have only two radio galaxies with measured [O III]λ5007/[O II]λ3727 (values ~3.3) and therefore a comparison is not really possible. Gelderman & Whittle (1994) also found that the [O III]λ5007 profiles in their CSS sources are broad and structured. The low dispersion of our spectra does not allow to say anything about this for our sample.

### 4.1. Reddening

The reddening of the emission line spectra has been estimated using the Balmer line ratios under the assumption of Case B recombination theory. The main ratio used for these estimates was Hγ/Hβ, for which we have a reliable value in three of our objects (0023-26, 1306-09 and 1934-638). In addition, we have measured Hδ/Hβ for 0023-26 and 1934-638 and Hα/Hβ for

**Table 3.** Emission-line fluxes and ratios

Line	$\lambda(\text{\AA})$	0023-26	0252-71	1151-34	1306-09	1814-63	1934-63	2135-20
MgII	2800	-	0.16±0.02	-	<0.12	-	-	0.43±0.04
[NeV]	3426	<0.04	0.08±0.02	-	<0.08	-	0.61±0.07	0.16±0.03
[OII]	3727	4.90±0.29	0.49±0.02	5.25±0.22	4.64±0.06	0.2:	3.12±0.07	2.97±0.05
[NeIII]	3869	0.51±0.04	0.12±0.01	-	0.60±0.05	-	1.44±0.06	0.90±0.04
[SII]	4072	0.23±0.02	0.07±0.02	-	0.15±0.04	-	0.95±0.05	0.23±0.04
H $\delta$	4101	0.11±0.02	0.06±0.02	-	0.16±0.04	-	0.22±0.05	0.09±0.04
H $\gamma$	4340	0.28±0.02	0.06:	-	0.33±0.04	-	0.41±0.06	0.38±0.04
[OIII]	4363	0.10±0.02	0.03:	0.64±0.16	0.06:	-	0.26±0.04	0.20±0.04
HeII	4686	<0.04	<0.04	<0.02	-	-	0.10±0.05	<0.16
H $\beta$	4861	1.0±0.04	-	1.0	1.0±0.07	-	1.0±0.09	1.0±0.06
[OIII]	4959	1.06±0.04	0.34±0.03	-	1.03±0.10	-	2.54±0.09	2.40±0.06
[OIII]	5007	3.40±0.04	1.0±0.03	21.88±4.6	3.57±0.11	1.0	7.21±0.11	7.44±0.08
[NI]	5200	0.21±0.04	-	-	-	-	0.18±0.04	0.25±0.07
[NII]	5755	<0.04	-	-	<0.08	-	0.12±0.03	-
[OI]	6300	2.70±0.09	-	-	-	0.4:	-	-
[NII]	6548	1.83±0.07	-	-	1.06:	-	-	-
H $\alpha$	6563	5.67±0.74	-	-	1.60:	4.2:	-	-
[NII]	6583	6.06±0.36	-	-	3.52:	-	-	-
[SII]	6716	2.48±0.44	-	-	-	-	-	-
[SII]	6731	3.10±0.42	-	-	-	-	-	-
H $\beta$ Flux		7.40 ± 0.25	26.30 ± 0.80	4.79±1.01	4.10 ± 0.40	19.3	6.39 ± 0.58	5.93 ± 0.37
		$10^{-16}$ ergs cm $^{-2}$ s $^{-1}$	[O III] $\lambda$ 5007 flux			[O III] $\lambda$ 5007 flux		

Note: columns (:): indicate values that are very uncertain.

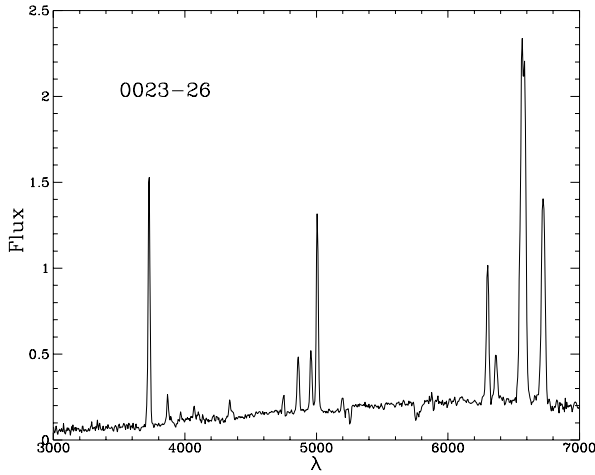


**Fig. 1.** Spectra of 0023-26. The wavelengths are in  $\text{\AA}$  and the flux scale is in units of  $10^{-16}$  erg cm $^{-2}$  s $^{-1}$   $\text{\AA}^{-1}$ . The spectra have been shifted in wavelength to the rest frames of the host galaxies.

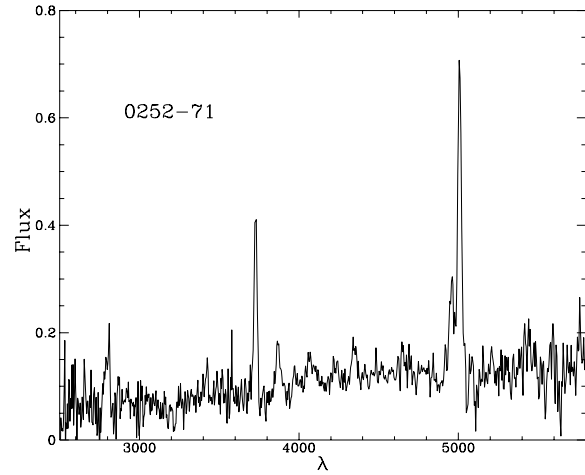


**Fig. 2.** Same as Fig. 1 for 0252-71.

0023-26 (for 1814-63 the quality of the data do not allow to measure any of these ratios).

The following values have been obtained for 0023-26:  $H\alpha/H\beta = 5.67 \pm 0.74$ ,  $H\gamma/H\beta = 0.28 \pm 0.02$ ,  $H\delta/H\beta = 0.11 \pm 0.02$  and respectively  $E(B - V) = 0.51 \pm 0.11$ ,  $1.18 \pm 0.16$ , and  $1.28 \pm 0.26$  (extinction law from Howarth 1983). The large discrepancy between the former and latter values could reflect the fact that the low resolution of our data, coupled with the poorer flux calibration at the red end of the spectrum intro-

duces a larger degree of uncertainty in the measurement of the  $H\alpha$  flux. Also, the  $H\alpha$  line is more likely to be affected by collisional excitation and line transfer effects than the higher order Balmer lines. For 1306-09 we obtain the following ratios:  $H\gamma/H\beta = 0.33 \pm 0.04$ ,  $H\delta/H\beta = 0.16 \pm 0.04$  and respectively  $E(B - V) = 0.80 \pm 0.30$  and  $0.75 \pm 0.35$ . Finally, for 1934-638 we obtain:  $H\gamma/H\beta = 0.41 \pm 0.06$ ,  $H\delta/H\beta = 0.22 \pm 0.05$  and respectively  $E(B - V) = 0.31 \pm 0.30$ , and  $0.26 \pm 0.26$ . On the other hand, for the ratio  $H\alpha/H\beta = 5.01$  given by Tadhunter (1987), we derive  $E(B - V) = 0.48$ .

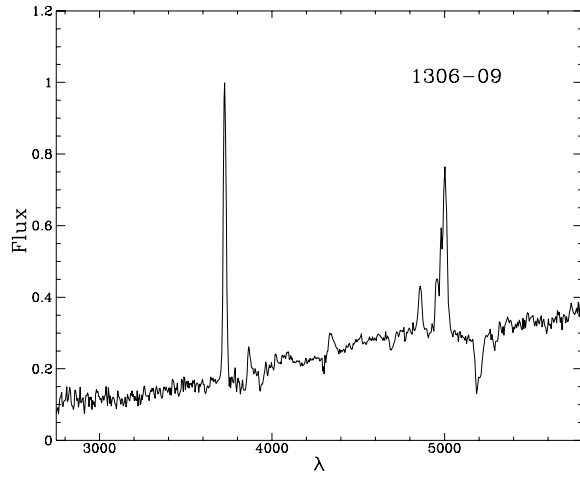


Fig. 3. Same as Fig. 1 for 1306-09.

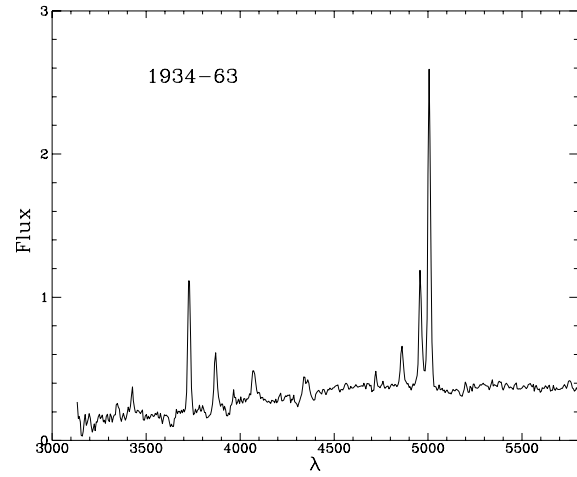


Fig. 5. Same as Fig. 1 for 1934-63.

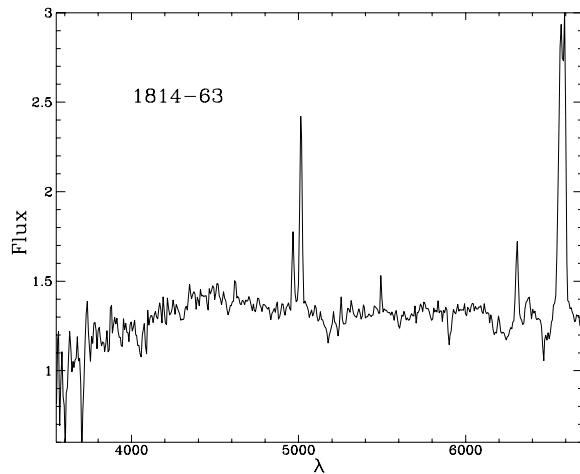


Fig. 4. Same as Fig. 1 for 1814-63.

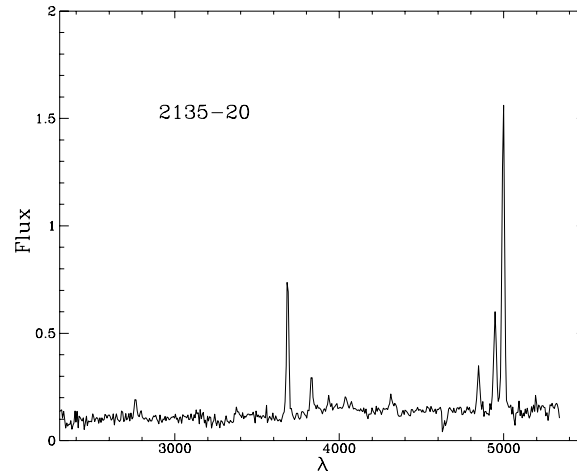


Fig. 6. Same as Fig. 1 for 2135-20.

Thus, there is evidence for substantial reddening in at least two (0023-26 and 1306-09) of the three CSS sources for which we have accurate measurements of the Balmer lines. Note, however, that reddening is also a feature of the dusty central regions of some extended radio sources (e.g. Cygnus A: Tadhunter *et al.* 1994b), so the CSS sources are not necessarily unusual in their reddening properties. Finally, it is worth noticing that in both the CSS sources with substantial reddening, the Galactic reddening (derived from both Burstein & Heiles 1984 and from the  $100\mu\text{m}$  maps in Rowan-Robinson *et al.* 1991) is low ( $E(B-V) \sim 0.02$ ) and the values derived above were corrected for the Galactic extinction.

#### 4.2. Temperature and density

Given the quality of our spectra, the gas temperature could be estimated only for 0023-26, 1934-63 and 2135-20. The values for 0252-71 and 1306-09 are too uncertain to derive a reliable value of the temperatures.

Using the temperature-sensitive diagnostic ratio  $R_{[\text{OIII}]} \equiv [\text{OIII}]4363/[\text{OIII}]5007$  and assuming the low density limit (and correcting for the reddening by using the  $H\gamma/H\beta$  given above), we obtain  $T \sim 18600K_{-600}^{+1000}$  for 0023-26,  $T \sim 20900K_{-1300}^{+2400}$  for 1934-63 and  $T \sim 17600K_{-2700}^{+1400}$  for 2135-20. In all cases the temperatures appear to be high and the value of 1934-63 confirms the early result by Penston & Fosbury (1978).

For one of the object in our sample (0023-26) it is possible to obtain a measurement for the density (although very uncertain) from the ratio of the density diagnostic  $[\text{S II}]\lambda\lambda 6717, 31$  lines. We find that the ratio of 6716/6731 is  $0.81 \pm 0.17$  which yields a density of  $1600 \pm_{780}^{2020} \text{cm}^{-3}$  for a temperature of 18600 K. In the case of 0023-26, we were also able to measure the ratio of the red and blue  $[\text{SII}]$  doublets. This ratio is 24.3, consistent with a range of densities from  $500 \text{cm}^{-3}$  at 13000 K to  $3200 \text{cm}^{-3}$  at 5000 K (Aller 1987). Thus, there is no evidence for high densities in 0023-26, such has been deduced on the basis of the transauroral  $[\text{SII}]$  ratios for 1934-63 (Fosbury *et al.* 1987).

**Table 4.** The D4000 parameter (Bruzual 1983) for the CSS sources with good quality spectra (see text for details) and the fraction of non-stellar light ( $F_{\text{ns}}$ ) below 4000Å (rest frame). In the last column are given the B-band polarization measurements or  $3\sigma$  upper limits

Object	D(4000)	$F_{\text{ns}}$	P(%)
0023-26	$1.34 \pm 0.04$	$0.67 \pm 0.04$	$<2.0$
1151-34	$1.02 \pm 0.07$	$0.98 \pm_{0.06}^{0.02}$	$<0.9$
1306-09	$1.41 \pm 0.07$	$0.60 \pm 0.07$	$6.3 \pm 1.3$
1934-63	$1.43 \pm 0.04$	$0.61 \pm 0.04$	$3.5 \pm 0.5$
2135-20	$1.10 \pm 0.05$	$0.90 \pm 0.05$	$<2.7$

### 4.3. The optical continua and polarisation

An analysis of the characteristics of the continuum has been done for the objects for which we have good quality spectra. The details about the modeling and study of the continuum are given in Dickson (1997). We find that all the CSS objects show an UV excess. To quantify the presence of this excess we have measured the parameter D4000 similarly to as described by Bruzual (1983). This parameter is derived as ratio of the mean flux in two, emission line free, continuum bins. Note that our definition of D4000 is different from that in the original Bruzual (1983) paper: in order to avoid serious contamination by emission lines, we have used the flux ratio of two 100Å wide bins centred on 3800Å and 4200Å. The measured values of D4000 can be compared with the theoretical value for a model of a passively evolving elliptical galaxy spectrum (Bruzual & Charlot 1993), assuming the initial mass function (IMF) from Salpeter (1955) and redshift of formation  $z_f = 5$ . From this comparison, it is possible to estimate the fraction of non-stellar light ( $F_{\text{ns}}$ ) below 4000Å (rest frame). D4000 and  $F_{\text{ns}}$  for the five CSS sources with good quality spectra are given in Table 4. Both 0252-71 and 1814-83 have been excluded from this Table because their continuum spectra are contaminated by respectively a foreground star and a foreground galaxy. All the remaining sources in Table 4 show clear evidence for a substantial UV excess.

Polarimetry has the potential to provide clues to the nature of the UV excess. B-band (rest-frame UV) imaging polarimetry has been obtained for 0023-26, 1306-09, 1934-63 (Tadhunter *et al.* 1994a) and 2135-20 (Shaw *et al.* 1995), while optical spectropolarimetry has been obtained for 1151-34 (Dallison, private communication). The polarization results are shown in the last column of Table 4, and it is clear that a variety of polarization characteristics are present in the sample. Significant polarisation has been detected in 1306-09 (6.3%) and 1934-63 (3.5%). In the case of 1934-69 the position angle of the electric vector is perpendicular to the radio axis while in the case of 1306-09 it is almost parallel. In the former case, scattered AGN light is the most likely polarization mechanism. In the other cases (i.e. 0023-26, 1151-34 and 2135-20) no polarization has been detected. Note that although the wavelength of the observations of 1151-34 is longer ( $\sim 5000\text{Å}$ ) than the B-band used for the other objects, this does not affect our result because the continuum is dominated by the non-stellar component.

The continuum properties of our small sample of CSS sources exactly mirror the continuum properties of the population of extended radio galaxies, which are also found to exhibit UV excesses and display a similar variety of polarization properties (see Tadhunter *et al.* 1997).

## 5. Comparison between CSS sources and the rest of the 2-Jy sample

In this section we will compare the luminosities and line ratios obtained for our sample of CSS sources with the values obtained for the rest of the 2-Jy sample described in Sect. 2. The rest of the sample consists of the extended radio sources together with some compact flat-spectrum quasars. The comparison with the rest of the 2-Jy sample (with  $\log P_{2.7 \text{ GHz}} > 26.0 \text{ W Hz}^{-1}$  to match the range in power of the CSS sources) will be done first by considering the emission lines that we were able to measure in all the objects (i.e. [O III]λ5007, [O II]λ3727), and then we will discuss some of the results obtained by considering faint diagnostic lines (i.e. He IIλ4686, [OIII]λ4363 etc.) which have only been measured in a subset of objects with good quality data.

### 5.1. The [OIII], [OII] emission lines

In Figs 7 and 8 the [O III]λ5007 and [O II]λ3727 line luminosities for the CSS sources are plotted together with the values for the rest of the 2-Jy sample (the flat spectrum sources are marked with different symbols in the figures). The CSS sources follow the same trend as the rest of the sample. However, it is worth noticing that, for a given radio power, they tend to be at the lower side of the [O III]λ5007 luminosity. A Kolmogorof-Smirnov test shows that this is only marginally significant (8%). A much larger sample of objects is required to verify this result. On the other hand, in the case of [O II]λ3727 there is no difference between the CSS and the other sources (see Fig. 8). This is consistent with the result obtained by Hes, Barthel & Fosbury (1996). Using narrow-band images taken in [O II]λ3727, they found that the distribution of the line luminosities of the CSS sources and their full sample (extracted from the 3CR) are not distinct.

As we discussed in the previous section, the ionization level shows a wide range for the CSS sources in our sample. Fig. 9 shows an histogram of the distribution of the [O III]λ5007/[O II]λ3727 ratio. The CSS source fall in the same range as the extended radio sources: although a couple of objects have a low ionization (i.e. a ratio [O III]λ5007/[O II]λ3727 < 1.0). However, low ionization states are also observed in some of the extended radio galaxies with similar radio power. The real nature of these low ionization objects is still uncertain and will be discussed in detail in (Tadhunter *et al.* 1997 in prep.). The value of [O III]λ5007/[O II]λ3727 for 1814-63 is very uncertain because of the problems already mentioned in Sect. 3, it should be therefore taken with caution.

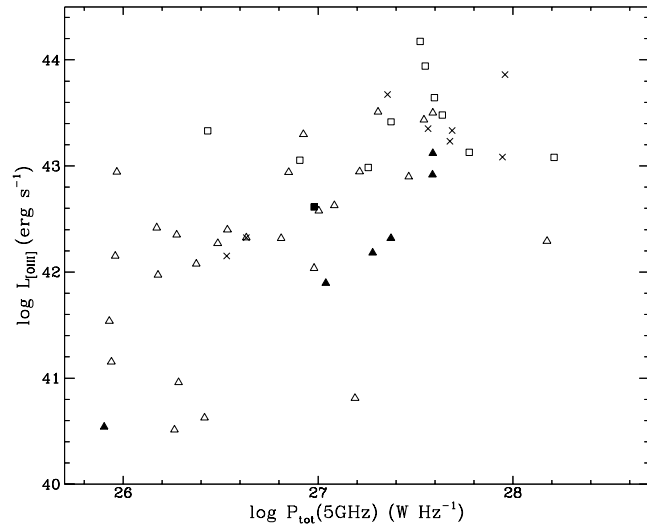


**Fig. 7.** Plot of the  $[\text{O III}]\lambda 5007$  luminosity versus the total radio power at 5 GHz. Triangles represent galaxies, squares represent quasars and filled symbols CSS sources. Crosses represent the flat spectrum sources

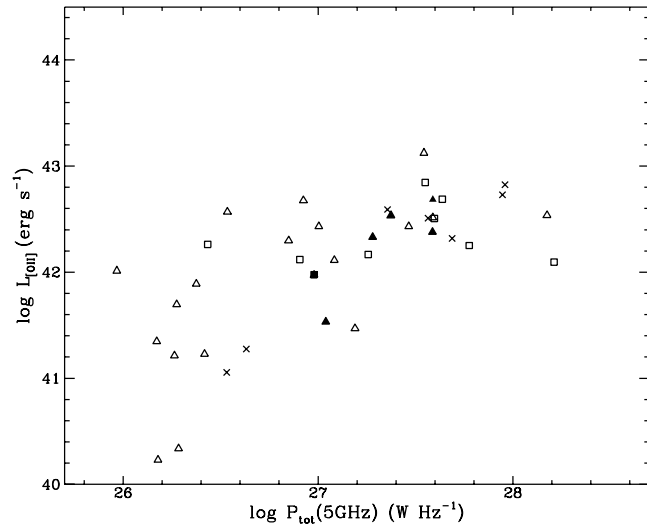


**Fig. 8.** Plot of the  $[\text{O II}]\lambda 3727$  luminosity versus the total radio power at 5 GHz. Triangles represent galaxies, squares represent quasars and filled symbols CSS sources. Crosses represent the flat spectrum sources

## 5.2. The diagnostic diagrams

Figs 10, 11 and 12 show three diagnostic diagrams. The data for 23 of the 2-Jy objects are shown together with the CSS sources (indicated by the black squares). For comparison, power-law photoionization models (Robinson *et al.* 1987) and shock models (Dopita & Sutherland 1996) are also plotted. The loci of the photoionization models are plotted with the solid lines (the index of the power law is shown in the plot). The shock models shown are from the precursor region (dashed line) and the shocked, cooling gas (region bounded by dot dashed line). Both shock models cover the range of shock velocity from 150 to 500

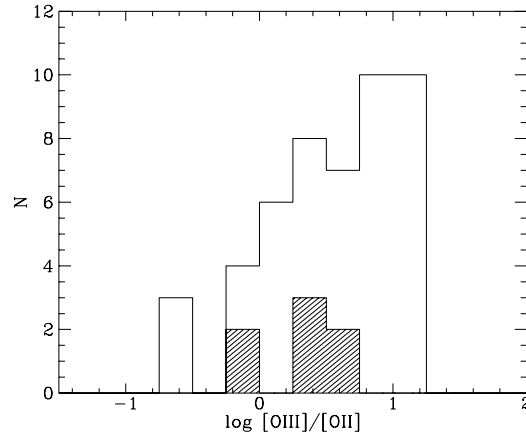


**Fig. 9.** Histogram of the distribution of the  $[\text{OIII}]/[\text{OII}]$  ratio. The shaded region represents the CSS sources.

$\text{km s}^{-1}$  and, in addition, the models of the shocked, cooling gas cover the range of magnetic field parameter  $0 < B/n^{1/2} < 4\mu\text{G cm}^{3/2}$ .

In all three diagnostics the CSS sources fall in the same region as the other objects.

Very good agreement between data and photoionization model is observed in the diagnostic diagram  $[\text{O III}]\lambda 5007/\text{H}\beta$  versus  $[\text{O II}]\lambda 3727/[\text{O III}]\lambda 5007$  (Fig. 10).

In Fig. 11 is plotted the temperature-sensitive ratio  $R_{[\text{OIII}]}$  versus  $[\text{O II}]\lambda 3727/[\text{O III}]\lambda 5007$ . Again, the CSS sources show similar values compared to the rest of the sample. The temperatures that follow from the  $R_{[\text{OIII}]}$  values are much higher than predicted by the *standard* power-law photoionization models, as can be seen by the discrepancy with the two lines that represent these models. This discrepancy is a well known problem for extended radio sources (Stasinska 1984, Tadhunter, Robinson & Morganti 1989) and a number of solutions have been proposed (Dopita & Sutherland, 1995; Binette, Wilson & Storchi-Bergmann 1996 and ref. therein). Among others, it has been often claimed that the small  $R_{[\text{OIII}]}$  is a consequence of unusual physical conditions (e.g. high density components) possibly connected with the presence of shocks as dominant ionization mechanism. Our finding that the values obtained for the temperature are not unique to CSS sources implies that similar conditions must exist in CSS and extended radio sources.

Finally, in Fig. 12 we present a plot of the  $\text{He II}\lambda 4686/\text{H}\beta$  versus  $[\text{O II}]\lambda 3727/[\text{O III}]\lambda 5007$ . The CSS sources show values similar to the rest of the sample although one of them has a particularly low value of  $\text{He II}\lambda 4686/\text{H}\beta$ . This diagnostic diagram shows a large scatter of the points. The data are better fitted by a power law with slope -2.0. This appears different from the results obtained for the  $[\text{O III}]\lambda 5007/\text{H}\beta$  versus  $[\text{O II}]\lambda 3727/[\text{O III}]\lambda 5007$  diagnostic diagram, where a power-law of index -1.5 provides a good fit to the data.

The discrepancies between the measured points and the models in Figs 11 and 12, suggest that AGN photoionization alone cannot explain the emission line spectra of the CSS

sources; it is probable that other mechanisms (e.g. autoionizing shocks: Sutherland *et al.* 1993) are required in addition to photoionization. However, similar statements could also be made about many of the extended radio sources, so once again the CSS sources are not unique in this aspect.

## 6. Discussion

From the above analysis we have found that the spectroscopic and polarimetric characteristics of the CSS sources are, to first order, similar to those of the extended sources of similar radio power and redshift. Among the parameters we have analysed, we find a marginal difference only in the  $[\text{O III}]\lambda 5007$  luminosity. (i.e. CSS sources showing lower  $[\text{O III}]\lambda 5007$  luminosity at a given radio power). It is clear that such spectral difference that might exist between the CSS and the extended radio sources is subtle, and will be revealed only by observations of larger samples of objects.

However, our results have important implications for our understanding of the nature of the CSS source phenomenon. For the case in which the emission line regions are predominantly photoionized by luminous AGN hidden in the cores of the galaxies, the observation of similar optical spectral properties for the extended and CSS radio sources provides strong evidence against the “frustration” hypothesis. As discussed in Fanti *et al.* (1995), the relatively large amount of material required in the central regions to confine the radio sources would imply a “trapping” density that would produce a much larger line luminosity than observed in our CSS sources and larger than for the extended radio sources. Moreover, we would expect the density of the gas to be enhanced by the jet/cloud interaction (leading to a lower ionization state) and the emission line luminosity to be enhanced by shocks.

We cannot exclude that, by chance, the jet in CSS sources is pointing toward high density regions. However, this is more likely to be the case for the minority of CSS sources showing a complex and/or asymmetric radio structure. For the sources in our sample (as well as in the symmetric objects studied by Fanti *et al.* 1995, see also their discussion about CSS morphology), the symmetry of the radio structure (as derived from the VLBI observations) does require a symmetric confining medium.

The only way to “save” the frustration idea in this case, is for the central ionizing illuminating source to be weaker in the CSS objects. However, unless the CSS sources form an entirely separate class of object, it is not clear why this should be the case.

On the other hand, if the emission line regions in the CSS sources are predominantly energised by their interaction with the radio jets, then the frustration scenario will also lead to larger emission line luminosities in the CSS sources than in the extended radio sources, since the interactions between the jets and the ISM must be stronger in the CSS sources in order to confine the radio sources.

Thus, whatever the ionization mechanism for the emission line gas, our optical spectra favour the idea that the CSS are genuinely young radio sources, rather than radio sources which

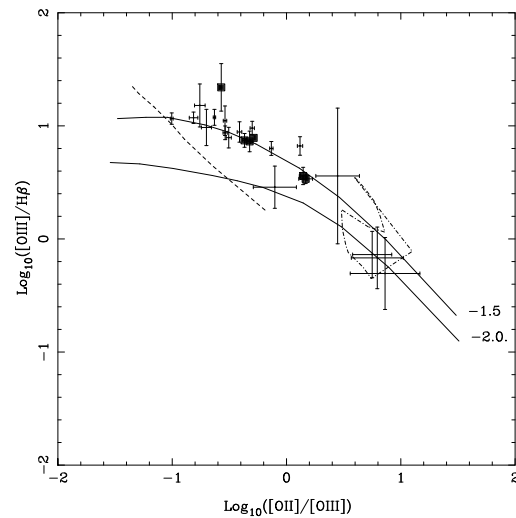


Fig. 10.

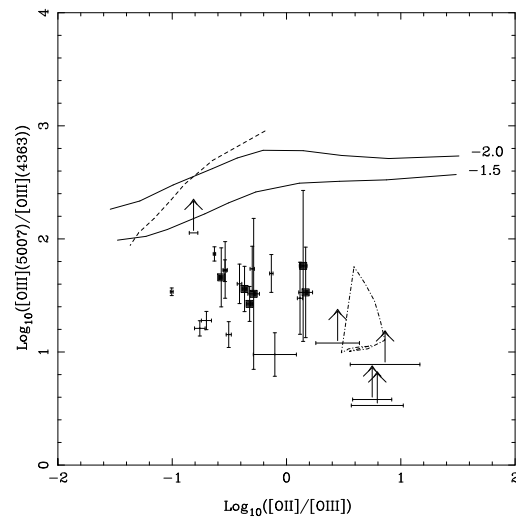


Fig. 11.

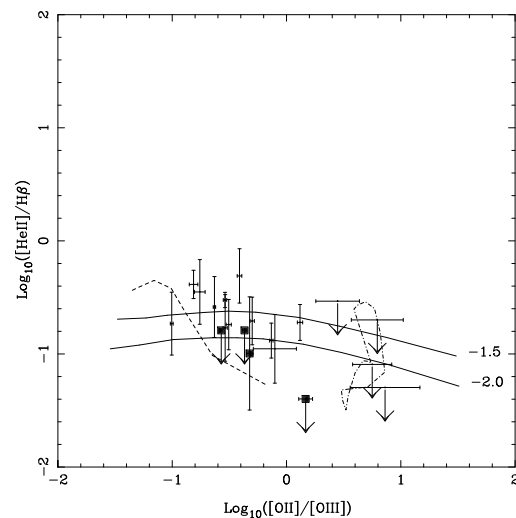


Fig. 12.

are confined by an unusually dense ISM in the cores of the galaxies.

## 7. Conclusions

We have presented long-slit spectra for a group of southern Compact-Steep-Spectrum (CSS) radio sources. The spectra are rich in strong emission lines (e.g. [O III] $\lambda$ 5007 and [O II] $\lambda$ 3727) as expected for such powerful radio sources. The line luminosities and ratios obtained for these compact sources have been compared with the rest of the southern 2-Jy sample. We found that the optical spectra for the CSS sources show characteristics very similar to the extended sources of similar radio power and redshift. In particular, we find that the CSS sources follow the correlation between the radio power and [O III] $\lambda$ 5007 and [O II] $\lambda$ 3727 luminosities found for the extended sources, although they seem to show lower [O III] $\lambda$ 5007 luminosity. Also in the optical polarimetry the CSS sources mimic quite well the variety of characteristics observed among the extended sources. The first-order similarity that we find is consistent with the idea that these are young radio sources in which the radio jets have yet to emerge from the central regions of the host galaxies.

## References

- Allen L. 1987, *Astrophys. Space Sci. Library* Vol. 112, Physics of Thermal Gaseous Nebulae, Reidel, Dordrecht
- van Breugel W.J.M. 1984. In Fanti, R., Kellerman, K.I., Setti, G. (eds.) *Proc. IAU Symp.* 110. Reidel Dordrecht p.59
- Binette L., Wilson A.S. & Storchi-Bergmann T. 1996, *A&A*, 312, 365
- Bruzual A.G. 1983, *ApJ*, 273, 105
- Bruzual A.G. & Charlot S. 1993, *ApJ*, 405, 538
- Burstein D., Heiles C. 1984, *ApJS*, 54, 33
- Cotton, W.D., Feretti, L., Giovannini, G., Venturi, T., Lara, L., Marcaide, J. & Wehrle, A.E. 1995, *ApJ*, 452, 605
- Dallacasa D., Fanti C., Schilizzi R.T., Spencer R.E., 1995, *A&A*, 295, 27
- Dickson R. 1997 PhD Thesis, University of Sheffield
- Dopita M.A. & Sutherland R.S., 1995, *ApJ*, 455, 468
- Fanti, R., Fanti, C., Schilizzi, R.T., Spencer, R.E., Nan Rendong, Parma, P., van Breugel, W.J.M., Venturi, T., 1990, *A&A*, 231, 333
- Fanti R. & Fanti C. 1994, in Bicknell G.V., Dopita M.A., Quinn P.J. eds., *1st Stromlo Symp. on the Physics of Active Galaxies*. ASP Conf.Ser. 54, San Francisco p. 341
- Fanti C., Fanti R., Dallacasa D., Schilizzi R.T., Spencer R.E. & Stanghellini C. 1995 *A&A*, 302, 317
- Fosbury R.A.E., Bird M.C., Nicholson W., Wall J.V. 1987 *MNRAS*, 225, 761
- Gelderman, R. & Whittle, M. 1994, *ApJS*, 91, 491
- Hes R., Barthel P.D., Fosbury R.A.E., 1996, *A&A* 313, 423
- Howarth I.D. 1983, *MNRAS*, 203, 301
- King *et al.* 1993, in *Subarcsecond Radio astronomy*, Davis R.J. and Booth R.S. eds., Cambridge University Press, p. 152
- King E., 1994, PhD Thesis, University of Tasmania
- King E. *et al.* , 1996, in *Extragalactic Radio Sources* Ekers R., Padrielli L., Fanti C., eds., p.75
- Morganti R., Killeen N, Tadhunter C., 1993, *MNRAS*, 263, 1023
- Morganti R., Tadhunter C.N., Fosbury R.A.E., Oosterloo T.A., Danziger I.J., di Serego Alighieri S., Siebert S., Brinkmann W., 1995, *Publ. Astr. Soc. Austr.*, 12, 3
- Morganti R., Oosterloo T., Reynolds J., Tadhunter C., Migenes V., 1997, *MNRAS*, 284, 541
- O’Dea, C.P., Baum, S.A. & Stanghellini, C., 1991, *ApJ* 380, 66
- Penston M.V. & Fosbury RAE 1978, *MNRAS* 183, 479
- Phillips T.J., Mutel R.L., 1982, *A&A* 106, 21
- Readhead A.C.S., Taylor G.B., Pearson T.J., Wilkinson P.N. 1996, *ApJ* 460, 634
- Readhead A.C.S. 1995, in *Quasars and AGN: High resolution Radio imaging*, Proc. Natl. Acad. Sci. USA, eds. Cohen M. and Kellerman K.I. Vol. 92, p. 11447
- Robinson A., Binette L., Fosbury R.A.E., Tadhunter C.N., 1987, *MNRAS*, 227, 97
- Rowan-Robinson M., Jones M., Leech K., Vedi K., Hughes J. 1991, *MNRAS*, 249,729
- Salpeter E.E. 1955 *ApJ*, 121, 161
- Shaw, M., Tadhunter, C., Dickson, R. & Morganti, R. 1995, *MNRAS*, 275,703
- Siebert J., Brinkmann W., Morganti R., Tadhunter C.N., Danziger J., Fosbury R.A.E., di Serego Alighieri S., 1996, *MNRAS*, 279, 1331
- Spencer, R.E., Schilizzi, R.T., Fanti, C., Fanti, R., Parma, P., van Breugel, W.J.M., Venturi, T., Muxlow, T.W.B., Nan Rendong, 1991, *MNRAS*, 250, 225
- Spencer R.E., McDowell J., Charlesworth M., Fanti R., Parma P. & Peacock J.A. 1989, *MNRAS* 240, 657
- Stasinska G. 1984, *A&A*, 135, 341
- Sutherland R.S., Bicknell, G.V., Dopita M.A. 1993, *ApJ*, 414,510
- Tadhunter C.N., Dickson R., Morganti R., Villar-Martin M. 1997 in “Quasar Hosts” ESO-IAC workshop in press
- Tadhunter C.N., Shaw M.A., Morganti R., 1994a, *MNRAS*, 271, 807
- Tadhunter C.N., Metz S., Robinson A. 1994b, *MNRAS*, 268, 989
- Tadhunter C.N., Morganti R., di Serego Alighieri S., Fosbury R.A.E., Danziger I.J., 1993, *MNRAS*, 263, 999
- Tadhunter C.N., Robinson A., Morganti R., 1989 In *ESO Workshop on Extranuclear Activity in Galaxies*, eds. Meurs E.J.A., Fosbury R.A.E., ESO Conf. and Workshop Proc. No.32, Garching, p.293
- Tadhunter, C.N. 1987, D.Phil. Thesis, University of Sussex
- Tzioumis *et al.* , 1996, in *Extragalactic Radio Sources* Ekers R., Padrielli L., Fanti C., eds., p.73
- Wall J., Peacock J., 1985, *MNRAS*, 216, 173
- Veron-Cetty M.P. & Veron P. 1993, “A Catalogue of Quasars and Active Nuclei” (6th Edition) ESO Sci. Rept.